Adaptive Controller for PMSGs of Grid-Connected Wind Turbines

OMAR AGUILAR, RUBEN TAPIA, CESAR SANTIAGO
Engineering Department
Universidad Politécnica de Tulancingo
Ingenierías #100, Col. Huapalcalco, CP. 43629, Tulancingo, Hidalgo, MÉXICO
ruben.tapia,[omar.aguilar],[cesar.santiago]@upt.edu.mx http://www.upt.edu.mx
J. MANUEL SAUSEDO
Centro de Investigación Avanzada en Ingeniería Industrial
Universidad Autónoma del Estado de Hidalgo
Carr. Pachuca- Tulancingo Km. 4.5, Pachuca, Hidalgo, MÉXICO
sausedos@uaeh.edu.mx http://www.uaeh.edu.mx

Abstract: - The wind energy boom in the world began in 1980's. This paper presents the modeling and control of a variable speed wind turbine system for low-power based Permanent Magnet Synchronous Generator is described. The currents from voltage-source converter are controlled in a synchronous orthogonal *dq* frame using a PI control tuning by a B-spline neural network. The B-spline neural network must be able to enhance the system performance and the online parameters updated can be possible. This paper proposes the use of adaptive PI controllers to maintain the current, frequency and DC link voltage constant. MATLAB and Simulink were employed for simulation studies. The simulations results confirm that the proposed algorithm is remarkably faster and more efficient than the conventional PI.

Key-Words: - Current control, distributed generation, voltage-source converter, neural network.

1 Introduction

During the last decades, renewable energies have experienced one the largest growth areas and wind energy becomes the most competitive. Actually doubly feed induction generators (DFIGs) are widely used as the generator in a variable speed wind turbine system. But, the DFIG needs a gearbox to match the turbine and rotor speed. The gearbox many times suffers from faults and requires regular maintenance, making the system unreliable. The reliability of the variable speed wind turbine can be improved significantly using a direct drive-based permanent magnet synchronous generator (PMSG). With gearless construction, such PMSG concept requires low maintenance, reduced losses and costs, and at the same time has high efficiency and good controllability [1].

Different arrays of wind energy conversion system (WECS) or distributed generation (DG) units utilize power electronic converters and, in particular, voltage-source converter (VSC) units, as the interface media with the utility grid [1]. For a grid connected DG unit, the interface VSC is conventionally controlled as a current controlled VSC (CC-VSC). Thus, direct-quadrature current components of the VSC are used to provide control of instantaneous real and reactive power exchange between the VSC and the grid [2].

A WECS is a physical system that has three primary components. The first one is rotor connected to blades. As wind goes through blades, it makes the rotor rotate and therefore creates mechanical power. The second one is a transmission that transfers power from the rotor to generator. The last one is electric generator that converts mechanical power to electric power [3].

The non-linear nature and wide range of operation requirements of the VSC impose considerable difficulty in the design of control systems [4]. The main techniques to regulate the VSC include either a variable switching frequency, such as the hysteresis control scheme, or fixed switching frequency schemes, such as the ramp comparison, stationary and synchronous frame proportional–integral (PI), optimal, nonlinear, adaptive and robust, predictive control, and soft computing or control techniques such as fuzzy control, neural networks control and on the fusion or hybrid of hard and soft control techniques [5].

The VSC synchronization is usually done by a phase-locked loop (PLL) system, as a good synchronization under balanced conditions or

ISBN: 978-1-61804-142-5

variations in electric grid. Nevertheless, having a good synchronization permits not only a good monitoring of the grid voltage phase and amplitude, or enhancing the capability of injecting power into the grid. A good PLL can provide further advanced functionalities to the control system, as it is the case of the islanding detection mode for wind farms.

In this paper a B-spline neural network (BSNN) is employed for two main tasks one for PI simultaneous tuning, taking care of a key feature: the proposed controller must be able to enhance the system performance; the second the online parameters updated can be possible. The strategy is proposed to update conventional PI parameters for currently operating in power converters that were tuned time ago.

2 Wind Energy Conversion System

2.1 PMSG Model

The PMSG is modeled under the following simplifying assumptions: sinusoidal distribution of stator winding, electric and magnetic symmetry, negligible iron, losses and unsaturated magnetic circuit. The voltage and electromagnetic torque equations of the PMSM in the *dq* reference frames are given by the following equations [6]:

$$v_d = -R_s i_d - L_d \frac{di_d}{dt} + L_q i_q \omega_s \tag{1}$$

$$v_q = -R_s i_q - L_q \frac{di_q}{dt} + \left(L_d i_d - \psi_m\right)\omega_s \tag{2}$$

where v_d and v_q are the *d-q* axis voltages, i_d and i_q are the *d-q* axis axis currents, R_s is the stator resistance, L_d and L_q are the *d-q* axis inductances, ω_s is the generator rotational speed, and ψ_m is the permanent magnetic flux.

Normally, the difference between the *d-q* axis mutual inductance is very small for a direct-driven multipole PMSG [6], and the stator winding resistance is much smaller than the synchronous reactance. Therefore, $T_e = p i_q \psi_m$.

2.2 Wind Turbine Model

The mechanical power extracted by a wind turbine from the wind is expressed by the cube law equation [6]

$$P_{wt} = 0.5\rho\pi R^2 v^3 C_p\left(\lambda\right) \tag{3}$$

$$\lambda = \frac{R\omega_l}{v} \tag{4}$$

where ρ is the air density, R is the blade length, ω_l is the rotor speed, v is the wind speed and $C_p(\lambda)$ is the turbine performance coefficient. The performance coefficient C_p is a function of the tip-speed-ratio λ (4). Using generator convention, the rotor speed and wind turbine driving torque follows from [6]

$$J\frac{d\omega_h}{dt} = \Gamma_{wt} - T_e - B\omega_h \tag{5}$$

$$T_e = p\left[\psi_m i_q + \left(L_d - L_q\right) i_d i_q\right] \tag{6}$$

where Γ_{wt} is the turbine driving torque referred to the generator ($\Gamma_{wt}=P_{wt}/\omega_l$), B is the active damping coefficient representing turbine rotational losses and p is the number of pole pairs.

3 Back-to-Back Converter Model

Fig. 1 illustrates that back-to-back converter system can be considered as the composition of two VSC systems: the right-hand side VSC system is a real reactive power and DC-voltage controller, and the left-hand side VSC system controlled the rotor speed. Fig. 1 shows the real-reactive power controller and the controlled DC-voltage power port are interfaced with grid and PMSG, respectively. The real-reactive-power controller and the controlled DC-voltage power port are connected in parallel from their DC-side terminals.

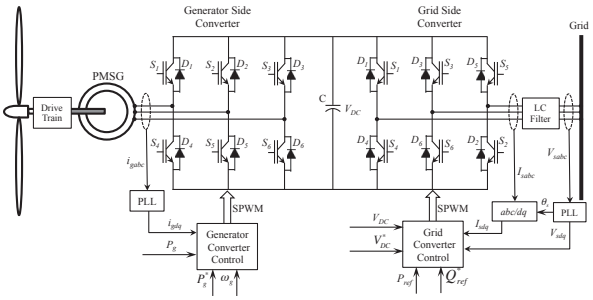

Fig. 1 Wind Energy Conversion System using PMSG.

3.1 VSC Dynamic Model

Fig. 1 shows the diagram of a three-phase three-wire VSC connected to the AC system represented by an equivalent Thevenin circuit via the inductance and resistance (L_T, R_T) of the interface transformer. The converter DC terminal is connected to a shunt capacitance (C_{dc}) and resistance (R_{dc}) representing the losses of the switching and affiliated components of the VSC. The three-phase AC side voltage balancing equations of the VSC are expressed [4] as:

$$L_S\frac{d\mathbf{I_{abc}}}{dt} + R_S\mathbf{I_{abc}} + L_T\frac{d\mathbf{I_{abc}}}{dt} + R_T\mathbf{I_{abc}} = \mathbf{V_{abc}} - \mathbf{V_{Tabc}} \tag{7}$$

where $\mathbf{I_{abc}} = [I_a \ I_b \ I_c]^T$ is the three-phase current vector, $\mathbf{V_{Sabc}} = [V_{Sa} \ V_{Sb} \ V_{Sc}]^T$ is the three-phase AC source voltage vector, $\mathbf{V_T} = [V_{Ta} \ V_{Tb} \ V_{Tc}]^T$ is the voltage source converter AC terminal three-phase voltage vector.

The rms amplitude $V_{tm}=m_o V_{dc}$ ($0<m_o<1$, related to the PWM modulation index), the frequency w and phase angle ø_T are controllable variables of the PWM voltage source converter. When connected to a constant frequency AC systems only $V_{tm}=m_o V_{dc}$ ($0<m_o<1$) and ø_T need to be used for the control of the VSC operation.

The dc-side voltage dynamic expression is deduced based on power balance between the ac and dc-side as

$$V_{dc}(t)\, I_{dc}(t) = P(t) - P_L(t) \tag{8}$$

where P(t) is the instantaneous real power at point of common coupling voltage, and P_L(t) includes the total power loss, and $P_{dc} = V_{dc} I_{dc}$ is the transferred power from the dc side to the "converter" system. Loss components include: a) capacitor dielectric loss, b) switching and on-state loss, and c) losses in the converter ac-side components as represented by R_{dc}. The DC current is:

$$C_{dc}\frac{dV_{dc}}{dt} = I_{dc} - \frac{V_{dc}}{R_{dc}} \tag{9}$$

rearranging all the other equations, the following system equations result:

$$\frac{d\mathbf{I_{abc}}}{dt} = \frac{1}{L_S + L_T}\left[-(R_S + R_T)\mathbf{I_{abc}} + \mathbf{V_{Sabc}} - \mathbf{V_T}\right] \tag{10}$$

$$\frac{dV_{dc}}{dt} = \frac{1}{C_{dc}}\left[-\frac{V_{dc}}{R_{dc}} + \mathbf{I_{abc}^T}\frac{\mathbf{V_T}}{R_{dc}}\right] \tag{11}$$

Using the orthogonal transformation, the tree-phase vectors in (10-11) are next converted to the *dqo*-frame. Thus by substituting the system state equations become:

$$\frac{d\mathbf{I}_d}{dt} = -aI_d + \omega I_q + bV_{sd} - bV_{Td} \tag{12}$$

$$\frac{d\mathbf{I}_q}{dt} = -\omega I_d - aI_q + bV_{sq} - bV_{Tq} \tag{13}$$

$$\frac{dV_{dc}}{dt} = \frac{1}{C_{dc}}\left[-\frac{V_{dc}}{R_{dc}} + \frac{1}{V_{dc}}\left(I_d V_{Td} + I_q V_{Tq}\right)\right] \tag{14}$$

where $a=(R_S+R_T)/(L_S+L_T)$, $b=(L_S+L_T)^{-1}$.

3.2 Instantaneous Reactive Power ($\alpha\beta$)

The α-β transformation is a useful tool for analyzing and modeling three-phase electrical systems. The main advantage of this representation is that a three-phase system can be represented graphically in two-dimension space (with only two variables), if the system is assumed balanced.

The power flow measurement may be done as follows:

$$S = (V_{t\alpha} I_{t\alpha} + V_{t\beta} I_{t\beta}) + j(V_{t\beta} I_{t\alpha} - V_{t\alpha} I_{t\beta}) \tag{15}$$

The real component of the complex power is the real or active power, while the imaginary part is the reactive power.

$$P = (V_{t\alpha} I_{t\alpha} + V_{t\beta} I_{t\beta}) \tag{16}$$

$$Q = (V_{t\beta} I_{t\alpha} - V_{t\alpha} I_{t\beta}) \tag{17}$$

3.3 Instantaneous Reactive Power (*d-q*)

The α-β or Clarke transformation offers advantages in the dimension order reduction. However, for feedback control implementation is highly desirable that the signals to be constant, not sinusoidal, and the α-β components are sinusoidal. This limitation is solved with the Park's transformation. The Park transformation has as input the α-β integrated vector with sinusoidal components.

Instantaneous real, reactive, and complex power components are expressed as [4],

$$S = (V_{td} I_{td} + V_{tq} I_{tq}) - j\,(V_{tq} I_{td} - V_{td} I_{tq}) \tag{18}$$

$$P = (V_{td} I_{td} + V_{tq} I_{tq}) \tag{19}$$

$$Q = (V_{tq} I_{td} - V_{td} I_{tq}) \tag{20}$$

Now, a key point of the Park transform is the angle θ, between the α-axis, which is static, and the *d* axis, which is turning at the line frequency with respect to the α-axis. The most widely accepted solution to provide synchronization between converters that inject energy coming from alternative supplies into the grid is a phase-locked loop (PLL) system. There exist a variety of PLL structures. The evaluation of the tangent β/α is the easiest way to estimate the angle θ [7].

4 Wind Turbine Control

4.1 Generator Side Converter Control

The generator side converter is controlled with a classical feedback control loop, as shown in Fig. 2. The control strategy uses a current control method in the *dq* synchronous reference frame and adjusts the generator speed to suit the wind speed. The speed control of the PMSG is realized on a rotating reference frame, where the rotational speed error is used as the input to a speed controller, which

ISBN: 978-1-61804-142-5

produces q-axis stator current command i_q desired.

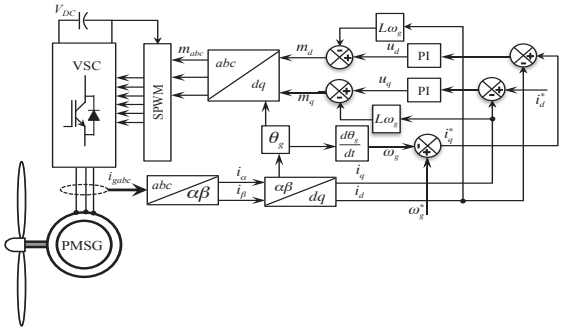

Fig. 2 Block diagram of generator side converter control scheme.

This reference is calculated from the optimal rotor tip speed ratio for getting maximum output power from each wind speed. To enhance the controller performance and get better results, the i_d and i_q currents are decoupled. The outputs from the two current controllers are the d and q-axis stator voltage references, which are sent to the sinusoidal pulse width modulation (SPWM) block. The SPWM will generate the switching signals required by the IGBT inside the converter.

4.2 Grid Side Converter Control

As the back-to-back converter decouples the generator and grid, the grid disturbances would not affect the operation of the generator-side converter. The control diagram is illustrated in Fig. 3. The grid-side converter control aim is to supply a reliable electric power to the consumers, following a specific set of parameters such as voltage, frequency and harmonic levels. The control scheme contains two cascaded loops. The inner loops independently control the grid i_d and i_q currents, while the outer loops control the DC-link voltage, the reactive and active power.

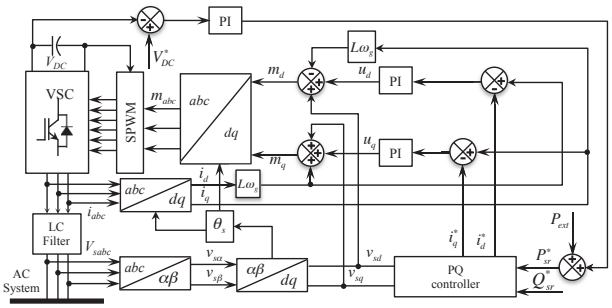

Fig. 3 Block diagram of grid side converter control scheme

The grid side converter has to keep the DC-link voltage constant and control the power factor of the output electricity by adjusting the reactive power. Under normal conditions the wind turbine's reactive power output is controlled under the range according to the grid codes.

This paper proposes the use of adaptive PI controllers to maintain the current and frequency AC load and DC link voltage constant, Fig. 3. We have three PI controllers that must be tuning to achieve the best back-to-back converter performance. Reactive power flow should be maintained close to zero. Both parameters the proportional and integer gains are updated online to attain a proper performance under different operating conditions, without restructuring the control scheme.

5 Controller Tuning

5.1 Neural Network Scheme

The proposed can be achieved adding a B-spline neural network to update k_P and k_I gains in the three PI controllers, Fig. 3, where each PI transfer function is given by,

$$\frac{U(s)}{E(s)} = \frac{k_I + k_p s}{s} \tag{21}$$

Thus, k_P and k_I are updated from a B-spline neural network at every sampled time. With this purpose, six artificial neural networks (ANN) are assembled in the control scheme.

A B-spline function is a piecewise polynomial mapping, which is formed from a linear combination of basis functions, and the multivariate basis functions are defined on a lattice [8]. The on-line B-spline associative memory network (AMN) adjusts its weights iteratively in an attempt to reproduce a particular function, whereas an off-line or batch B-spline algorithm typically generates the coefficients by matrix inversion or using conjugate gradient. The B-spline neural networks (BSNN's) output can be described by [8],

$$y = \mathbf{a}^T \mathbf{w} \tag{22}$$

$$\mathbf{w} = \begin{bmatrix} w_1 & w_2 \ldots & w_\gamma \end{bmatrix}^T ; \mathbf{a} = \begin{bmatrix} a_1 & a_2 \ldots & a_\gamma \end{bmatrix}^T \tag{23}$$

where w_i and a_i are the i-th weight and the i-th BSNN basis function output, respectively; γ is the number of weighting factors.

In this paper it is proposed that k_P and k_I be adapted through one BSNN, respectively, for the

ISBN: 978-1-61804-142-5

grid voltage source converter. The determination of parameters control is made based on the close relationship between controllers and gains performance. Then the dynamic control parameters for back-to-back system can be described as follows:

$$k_P = NN_m\left(e_x, w_m\right) \tag{24}$$

$$k_I = NN_m\left(e_x, w_m\right) \tag{25}$$

where NN_m denotes the B-spline network which is used to calculate k_P and k_I; w_m is the corresponding weighting factor; m=1,2,3 number of PI controllers. Fig. 4 depicts a scheme of the proposed BSNN.

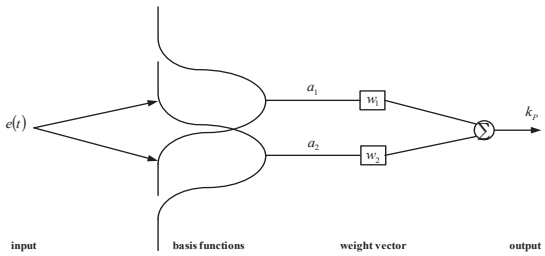

Fig. 4. Proposed BSNN for adapting K_P and K_I control parameters.

5.2 Learning rule

Learning in artificial neural networks is usually achieved by minimizing the network's error, which is a measure of its performance, and is defined as the difference between the actual output vector of the network and the desired one.

In this paper, the neural network is trained on-line using the following error correction instantaneous learning rule [9],

$$w_i(t) = w_i\left(t-1\right) + \frac{\eta e_i\left(t\right)}{\left\|\mathbf{a}(t)\right\|_2^2} a_i(t) \tag{26}$$

where η is the learning rate and e_i(t) is the instantaneous output error. Respect to the learning rate, it takes as initial value one point within the interval [0, 2] due to stability purposes [8]. This value is adjusted by trial-and-error. If η is set close to 0, the training becomes slow.

It is proposed that during the actualization procedure, a dead band is included to improve the learning rule convergence. The weighting factors are not updated if the error has a value below 0.1%,

$$w_i(t) = \begin{cases} w_i\left(t-1\right) + \dfrac{\eta e_i\left(t\right)}{\left\|\mathbf{a}(t)\right\|_2^2} a_i(t), \text{if } \left|e_i\right| > 0.0001 \\ w_i\left(t-1\right) \quad \text{otherwise} \end{cases} \tag{27}$$

This learning rule has been elected as an alternative to those that use, for instance, Newton's algorithms for updating the weights [9] that require Hessian and Jacobian matrix evaluation. Regarding the weights' updating (27) should be applied for each input-output pair in each sample time; the updating occurs if the error is different from zero. That is the reason because it is said that the weights converge to optimal values [8]. Hence, the BSNN training process is carried out continuously on-line, while the weights' values are updated using only two feedback variables.

6 Test Results and Analysis

In order to demonstrate the feasibility of this proposition, a wind generation system is employed. Matlab-Simulink are used for simulation, the proposed tuning performance is exhibited. To analyze the results, simulations are developed under different scenarios with PI controllers tuned by BSNN (dynamic parameters). Some operating conditions are taken into account. The models of the low-power (3-kW) rigid drive train PMSG based WECS shown in Fig. 1 are included in the simulations.

Major system parameters are listed in Table 1. The power converter and the control algorithm are also implemented and included in the model. The sampling time used for the simulation is 20 μs.

Table 1
Parameters of PMSG wind power system.

Blade length:	R=2.5 m
Multiplier ratio:	i=7
Efficiency	η=1
HSS inertia:	J=0.5042 kg m^2
No. of poles	p=3
Stator inductance	L_d=L_q=41.56 mH
Magnet flux linkage	ψ_m=0.4382 Wb
Rated Voltage	380 volts

The wind speed profile is considered varying smoothly with step rate at different slopes, as see in Fig. 5. The system is subjected to the following sequence of events: until t = 0.033 s, Pref = 2200 W Qsref ≡ 0. At t = 0.033 s, Psref is subjected to a step change from 2200 to 2700 W. At t = 0.66 s, Psref is subjected to another step change from 2700 to −1800 W.

Fig. 6 shows the simulation result of DC link voltage with the proposal and considering fixed parameters. Fig. 6 exhibits the dynamic behavior of the reactive power at DC link bus, where the proposed scheme is worked. The transient response

is diminished in terms of overshot magnitude without parameters update. The adaptive neural network PI exhibits very well performance adapting itself to the new conditions. Fig. 7 Illustrates that P_s and Q_s rapidly track P_{ref} and Q_{ref} , respectively.

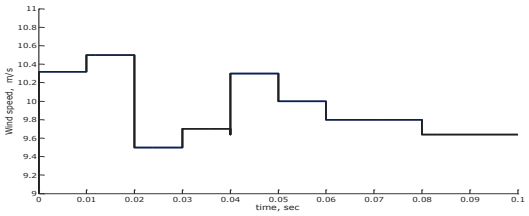

Fig. 5. Wind speed variation in m/s.

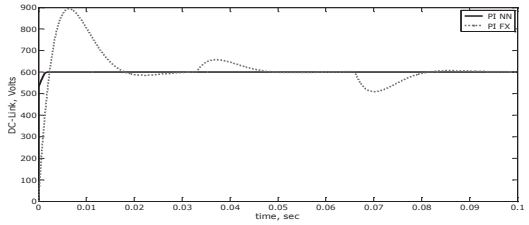

Fig. 6. DC link voltage performance.

Fig. 8 shows the instantaneous load currents when the load changes. The load current is changing with the load variations as expected. From Fig. 8, it is seen that there is no significant rise in the current waveform during load transient.

Fig. 9 displays the proportional an integral gain's evolution for controller one. Quite similar results are exhibited for all adaptive parameters.

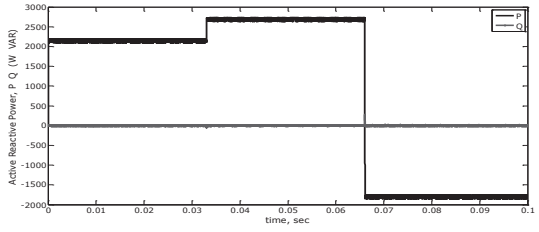

Fig. 7. Active and reactive power in WECS terminals.

7 Conclusion

This paper is aimed to exhibit the performance of a variable speed wind turbine system for low power based Permanent Magnet Synchronous Generator, which feeds an AC power grid. In order to attain such purposes a B-spline Neural Network-based control is proposed. We can see from the simulation results that the system with the proposed control method has a stable operation at various load conditions.

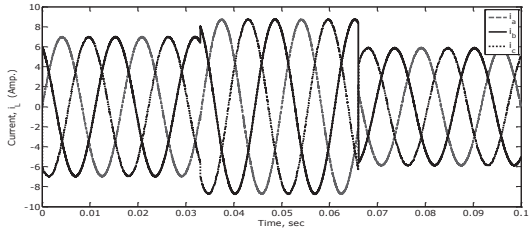

Fig. 8. Instantaneous output line current.

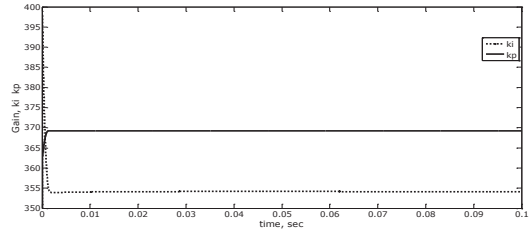

Fig. 9. Proposed BSNN for adapting k_i and k_p parameter, controller 1.

Acknowledgement

The authors thank PROMEP under Grant Redes Temáticas de Colaboración.

References:

[1] Bin Wu, Yongqiang Lang and Samir Kouro "*Power Conversion and Control of Wind Energy Systems*," USA: IEEE Press, 2011.

[2] K. Dai, P. Liu, Y. Kang, and J. Chen, "Decoupling current control for voltage source converter in synchronous rotating frame," *4th IEEE Int. Conf. Power Electronics Drive Systems*, Vol. 1, 2001, pp. 39–43.

[3] Ackermann T., *Wind Power in Power Systems*. England: Wiley, 2005.

[4] J. Arrillaga, Y. Liu, N. Watson and N. Murray, *Self-Commutating Converters for High Power Applications*. United Kingdom: Wiley, 2009.

[5] Hoa M. Nguyen, D. Subbaram Naidu, "Advanced Control Strategies for Wind Energy Systems: An Overview", 2011 IEEE PES Power Systems Conference & Exposition.

[6] I. Munteanu, A. Iuliana B., N. A. Cutululis, E. Ceanga, *Optimal control of Wind Energy Systems*, Springer, 2008.

[7] Remus Teodorescu, Marco Liserre and Pedro Rodríguez, *Grid Converters for Photovoltaic and Wind Power Systems,* Wiley, 2011.

[8] Brown, and C. Harris, *Neurofuzzy Adaptive Modelling and Control*, Prentice Hall International, 1994.

[9] David Saad, "*On-line learning in neural networks*," Cambridge University Press 1998.